DESIGN, VOLTAGE MODE CONTROL AND NON-IDEAL ANALYSIS OF A LOW VOLTAGE-HIGH CURRENT SYNCHRONOUS BUCK CONVERTER

Baris YILDIZ[1], Gokhan ALTINTAS[1], Mehmet Onur GULBAHCE[1], Derya Ahmet KOCABAS[1]

[1]Department of Electrical Engineering, Faculty of Electrical and Electronics Engineering, Istanbul Technical University, Istanbul, Turkey
barisyildiz93@gmail.com, altintasgo@itu.edu.tr, ogulbahce@itu.edu.tr, derya.kocabas@itu.edu.tr

Abstract: *Synchronous and non-synchronous buck converters are uninsulated DC-DC converters which are widely used in any application that needs low voltage and high current. In ideal case, switches are accepted as ideal during simulations of these converters in order to simplify the analysis. Non-ideal case can be analyzed by adding the resistances of switches and inductances as components to simulation. In this study, steady state and transient state are both analyzed for non-ideal case for continuous conduction mode by designing a 225 W synchronous buck converter. Simulations are performed in MATLAB/Simulink by calculated design parameters. A digital PI controller was designed according to simulation results in order to control the output voltage. Stability analysis for the designed converter was achieved. In the second part of the study, converter was manufactured and designed controller was embedded to a DSP based microcontroller. The performance of the system was investigated by testing the designed circuit under variable load and input voltage conditions and a comparison between simulation results for non-ideal case and practical results was made.*

Keywords: *Switch-mode power supply, converter, synchronous buck, transient state, steady state, stability, C2000 Piccolo LaunchPad.*

1. Introduction

In recent years, the importance of DC-DC converters is increased due to their high efficiency, low-cost, small dimensions and lower-loss than that of linear voltage regulators. Increasing demand of portable electronic industry necessitated the improvements of switched DC-DC converters and their control systems [1, 2]. Two of the most basic samples for this converters are synchronous and asynchronous buck converters given in Figure 1 those can be transformed into the other one.

The main switch Q_1 in the circuit topology that is placed in the upper position is called semi-conductor power switch and input voltage is decreased proportionally to the duty cycle of this switch. The other components in the topology are output inductor L and output capacitor C. While there is one power-diode (D_1) in an asynchronous buck-converter, this switch is replaced by a controlled semi-conductor power switch (Q_2) in a synchronous buck converter. These two switches positioned one under the other are switched synchronously in a way to complement each other [3,4].

Synchronous buck converters (SBC) began to take the place of conventional buck-converters in most of the applications. Especially, the need of low-voltage, high-current power systems is increased as the number of portable electronic applications increased [5].

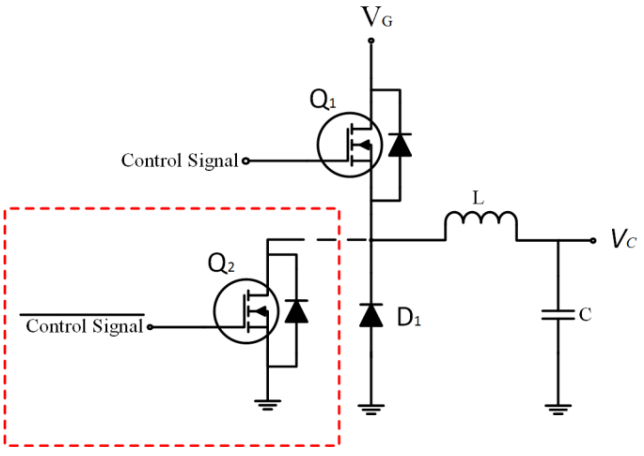

Received on: 16.06.2017
Accepted on: 06.07.2017

Figure 1. Buck Converter (It becomes synchronous type when D_1 diode is replaced with Q_2 switch)

Duty ratio is low in buck converters where the output voltage is significantly reduced with regard to input voltage. In this situation, current passes through the power diode for a longer time and efficiency is reduced by increased losses over the diode. There are studies [6] where the efficiency is increased by replacing the diode with a MOSFET in low-frequency applications. The lower conduction resistance of semi-conductor switch that is used instead of the diode provides the synchronous buck converters to be more efficient than conventional buck converters below certain current levels. But when it comes to very high current values, it must be taken into account that the topology can lose its advantage of efficiency, since the conduction losses of the semi-conductor power switch becomes greater than that of the diode.

The most important advantage of SBC is that the voltage-drop in forward mode over controlled semi-conductor switch placed below the other is less than that of the diode used in an asynchronous buck converter and that lower loss is produced consequently [7].

Another advantage of SBC to asynchronous buck converters is that it can keep the output voltage constant at the reference voltage value when it is controlled by a robust control algorithm even in no-load operation. But in no-load operation, inductance current flows from the capacitor to the switch, not from the switch to capacitor, since the synchronous switch turns on to adjust the output voltage and power loss is created over the resistance of the inductance and conduction resistance of the semi-conductor switch. Therefore, being able to control the output voltage when there is no-load brings about small amounts of losses. In literature, there are studies about the control of synchronous buck converters [8, 9].

In open-loop operation, the output voltage is reduced by increasing load current, since non-ideal the switches in both converter topologies creates voltage drop and losses. Therefore, in applications where the output voltage is desired to be constant, output voltage needs to be controlled for different loading conditions by a controller [10-12]. In non-ideal operation, conduction resistance of the semi-conductor switches or voltage drop at loaded operation, resistance of inductance winding and equivalent series resistance of the capacitor must be taken into account.

This study complements a previous study and extends the limits of previous work [13]. In previous part [13], a synchronous buck converter is designed having a power of 225 W and an output voltage of 0-30 V to be used in low-voltage, high-current applications. In this study, steady-state analysis of the circuit is performed for continuous current mode by both simulations and analytical calculations. General small signal analysis for buck converters is extended for synchronous type unlike previous studies. Transfer functions from "input-to-output" and from "control signal-to output" are both obtained and given. A conventional discrete PI controller is designed for controlling the output voltage and all controller, converter simulations are built in MATLAB/Simulink. The controller is embedded to C2000 Piccolo LaunchPad which is a digital signal processing based microcontroller and output voltage control is provided. Stability analysis of the designed controller is another extension of the study by same authors. Additionally, the performance of the designed power electronic converter together with the controller is examined under variable load and variable input voltage conditions and compared results are presented.

2. Steady State Analysis of SBC

Inductor current and capacitor voltage are periodic signals when the converter operates in steady state mode and their mean values are zero. Steady state analysis of the converter can be divided into two sub-intervals by assuming ripple amplitudes of the voltage of the inductance and the current of the capacitor are almost zero. The first sub-interval is "Q_1 is on, Q_2 is off" stage and the second sub-interval is "Q_2 is on, Q_1 is off" stage [12].

- Q_1 on, Q_2 is off;

Figure 2 shows the equivalent circuit of the first sub-interval where the Q_1 is on, Q2 is off and the equations are written from the circuit in Figure 2. In the equations parameters are D duty ratio, T switching period, f switching frequency, V_g input voltage, R_L inductor parasitic resistor, r_{dson} on-state resistance of switching component, V_L inductor voltage, V_C capacitor and output voltage of converter, i_C capacitor current, I_L inductor current, R_{Load} load resistor.

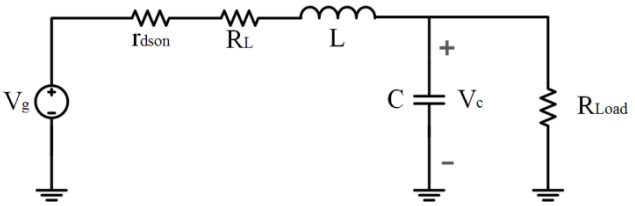

Figure 2. First subinterval equivalent circuit of the SBC

$$V_L = V_g - V_C - I_L(r_{ds_{on}} + R_L) \quad (1)$$

$$i_C = I_L - \frac{V_C}{R_{Load}} \quad (2)$$

- Q1 off, Q2 is on;

Figure 3 shows the equivalent circuit of the first subinterval where the Q_1 is off, Q_2 is on and the equations are written based on the circuit.

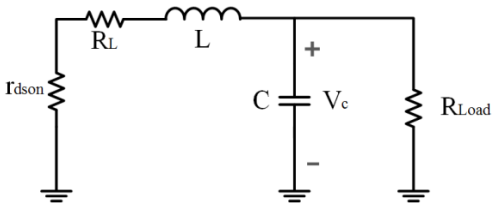

Figure 3. Second subinterval equivalent circuit of the SBC

$$V_L = -V_C - I_L(r_{ds_{on}} + R_L) \quad (3)$$

$$i_C = I_L - \frac{V_C}{R_{Load}} \quad (4)$$

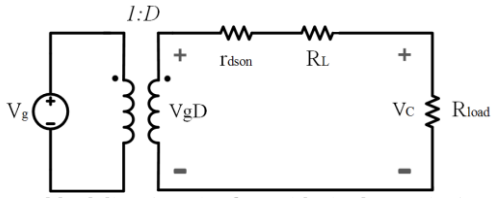

1 blank line (9-point font with single spacing)

Figure 4. Equivalent circuit of the converter with DC transformer

1 blank line (9-point font with single spacing)

Relation between input voltage and output voltage is obtained by solving the circuit which is given in Figure 4 and (5) indicates the output voltage value in terms of circuit parameters.

$$V_C = \frac{R_{Load}}{R_{Load} + r_{ds_{on}} + R_L} \cdot D \cdot V_g \quad (5)$$

Converter power, input voltage, output voltage, switching frequency, ripples of both current and voltage are the main concerns for design of the converter. Regarding to these values, filter and switching components are determined. IRFZ44N is chosen as MOSFET. Converter parameters are listed in Table 1.

Table 1. Converter parameters

Parameters	Notation	Value
Rated input voltage	V_g	30 V
Rated output voltage	V_C	15 V
Rated load current	I_L	15 A
Inductor parasitic resistor	R_L	0.118 Ω
MOSFET resistor(IRFZ44N)	r_{dson}	0.035 Ω
Inductor current ripple	ΔI_L	0.34 A
Output voltage ripple	ΔV_C	0.3 mV
Output capacitor	C	1000µF
Output inductor	L	142µH
Switching frequency	f_s	150 kHz

Small Signal Analysis of SBC

Power electronic circuits contain both AC and DC signals. Therefore, these converters must be analysed in the way of small signal. Small signal analysis is also named as AC analysis and dynamics response of the converter is obtained by AC analysis. This is done to see the effects of input voltage, duty ratio and load current on output voltage. These signals include ripples as shown in Figure 5. In the steady state analysis, AC components (so ripples) are ignored. Ripples are determined by inductor current and capacitor voltage and this affects duty ratio D instantly. In this analysis, ripple value of duty ratio D is stated as d.

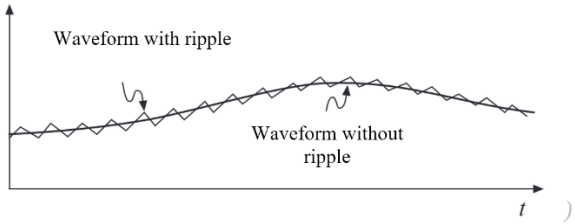

Figure 5. Waveforms with and without ripple

Small signal analysis can be done through state space model and canonical model methods or by accepting there are small ripples around average value [14]. DC and AC components can be analysed with state space method [14]. In general, equations which are written according to equivalent circuits are formed into matrix form, and inductor and capacitor parameters are indicated as state variables. Values of state variables and output values depend on mostly previous values of them, not only on instant values. State space model is mainly expressed in (6) and (7), where u indicates source, y output, x state variables. K, A, B, C and E are constant coefficient matrices [14].

$$K\frac{d}{dt}x(t) = A.x(t) + B.u(t) \quad (6)$$

$$y(t) = C.x(t) + E.u(t) \quad (7)$$

In the investigated converter output signal y(t) must be output voltage v and input signal u(t) must be input voltage vg. State variables of the system are inductor current (i_L) and capacitor (output) voltage (v_c or v) and they are inserted to (6) and (7). Circuit has two sub-intervals thus the coefficient matrices of the state space model are different from each other. Duty ratios are also different in the sub-intervals so the coefficient matrices have different values like A_1, A_2, B_1, B_2, C_1, C_2, E_1, E_2. When the two sub-interval models are merged, total coefficients for both intervals (A, B, C, E) are calculated by averaging these matrices according to duty ratio D and the complement of it D' as in (8), (9), (10), (11). K has no dependency on duty ratio, since it is the values of the inductor and capacitor [14].

$$A = DA_1 + D'A_2 \quad (8)$$

$$B = DB_1 + D'B_2 \quad (9)$$

$$C = DC_1 + D'C_2 \quad (10)$$

$$E = DE_1 + D'E_2 \quad (11)$$

Since steady state values are constant, differentiated averaged matrices are equalled to zero to obtain steady state values as given below;

$$0 = AX + BU \quad (12)$$

$$Y = CX + EU \quad (13)$$

AC signals are analysed as in (14) and (15) [14]:

$$K\frac{d}{dt}x(t) = Ax(t) + Bu(t) + [(A_1 - A_2)X + (B_1 - B_2)U]d(t) \quad (14)$$

$$y(t) = Cx(t) + Eu(t) + [(C_1 - C_2)X + (E_1 - E_2)U]d(t) \quad (15)$$

According to (14) and (15), transient analysis of the converter in the two sub-intervals is completed. (16) and (17) show the re-arrangement of the (6) and (7) for the non-ideal case.

-First sub-intervals:

$$L\frac{di(t)}{dt} = v_g(t) - v(t) - i(t).(r_{DS_{on}} + R_L) \quad (16)$$

$$C\frac{dv(t)}{dt} = i(t) - \frac{v(t)}{R} \quad (17)$$

State space representation of the (16) and (17) are given in (18) and (19).

$$K\frac{d}{dt}x(t) = \begin{bmatrix} -(r_{ds_{on}} + R_L) & -1 \\ 1 & -\frac{1}{R} \end{bmatrix}.x(t) + \begin{bmatrix} 1 \\ 0 \end{bmatrix}.u(t) \quad (18)$$

$$y(t) = \begin{bmatrix} 0 & 1 \end{bmatrix}.x(t) + [0].u(t) \quad (19)$$

Equation coefficient matrices are as in (20), (21), (22) ve (23).

$$K = \begin{bmatrix} L & 0 \\ 0 & C \end{bmatrix} \quad (20)$$

$$A_1 = \begin{bmatrix} -(r_{ds_{on}} + R_L) & -1 \\ 1 & -\frac{1}{R} \end{bmatrix} \quad (21)$$

$$B_1 = \begin{bmatrix} 1 \\ 0 \end{bmatrix} \quad (22)$$

$$C_1 = \begin{bmatrix} 0 & 1 \end{bmatrix} \quad (23)$$

$$E_1 = [0] \quad (24)$$

-Second sub-intervals:

$$L\frac{di(t)}{dt} = -v(t) - i(t).(r_{ds_{on}} + R_L) \quad (25)$$

$$C\frac{dv(t)}{dt} = i(t) - \frac{v(t)}{R} \quad (26)$$

State space representation of the (25) and (26) are given in (27) and (28).

$$K\frac{d}{dt}x(t) = \begin{bmatrix} -(r_{ds_{on}} + R_L) & -1 \\ 1 & -\frac{1}{R} \end{bmatrix}.x(t) + \begin{bmatrix} 0 \\ 0 \end{bmatrix}.u(t) \quad (27)$$

$$y(t) = \begin{bmatrix} 0 & 1 \end{bmatrix}.x(t) + [0].u(t) \quad (28)$$

Equation coefficient matrices are as in (29), (30), (31) ve (32).

$$A_2 = \begin{bmatrix} -(r_{ds_{on}} + R_L) & -1 \\ 1 & \frac{-1}{R} \end{bmatrix} \quad (29)$$

$$B_2 = \begin{bmatrix} 0 \\ 0 \end{bmatrix} \quad (30)$$

$$C_2 = \begin{bmatrix} 0 & 1 \end{bmatrix} \quad (31)$$

$$E_2 = [0] \quad (32)$$

With the equations obtained from two sub-intervals, (33) is derived from (14), (34) is derived from (15). (vc(t)=v(t))

$$L\frac{di(t)}{dt} = -v(t) - i(t)(r_{ds_{on}} + R_L) + D.v_g(t) + V_g.d(t) \quad (33)$$

$$C\frac{dv(t)}{dt} = i(t) - \frac{v(t)}{R} \quad (34)$$

AC equivalent circuit representing (33) and (34) is shown in Figure 6.

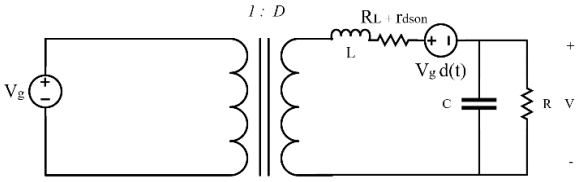

Figure 6. Small signal equivalent circuit

There are two inputs in the converter as shown in the model in Figure 6. One of them is the input voltage (V_g), the other one is duty ratio (d). By (33) and (34), equivalent circuit transfer functions can be written.

3.1. Transfer Function From Input to Output

To obtain input to output transfer function, the effects of other inputs are assumed to be zero. Thus, when d(t) is assumed to be zero, the equivalent circuit given in Figure 7 where primary side referred to the secondary side is obtained.

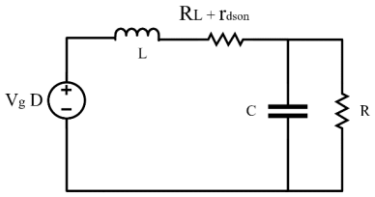

Figure 7. Input to output equivalent circuit

The solution of the above circuit includes the solution of differential equations. These differential equations are solved by Laplace transformation and transfer function is derived as given in (35).

$$G_{v_g}(s) = \frac{D.R}{R+(r_{ds_{on}}+R_L)+s(L+R.C.(r_{ds_{on}}+R_L))+R.L.C.s^2} \quad (35)$$

Transfer function from input voltage to output voltage is obtained in (39) when the (36), (37) and (38) are substituted into (40).

$$G_{v_0} = \frac{D.R}{R+(r_{ds_{on}}+R_L)} \quad (36)$$

$$w_0 = \sqrt{\frac{R+(r_{ds_{on}}+R_L)}{R.L.C}} \quad (37)$$

$$Q = \frac{\sqrt{R.L.C.(R+r_{ds_{on}}+R_L)}}{L+R.C.(r_{ds_{on}}+R_L)} \quad (38)$$

$$G_{v_I}(s) = \frac{G_{v_0}}{1+\frac{s}{Qw_0}+\frac{s^2}{w_0^2}} \quad (39)$$

3.1. Transfer Function From Control Signal to Output

Control signal of the converter is the duty ratio. Similar to Section 3.1, parameters including input voltage are set to zero. Circuit model is given in Figure 8.

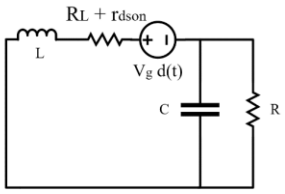

Figure 8. Control to output equivalent circuit.

If the circuit equations are transformed by using Laplace transformation, (40) is derived.

$$G_{vd}(s) = \frac{V_g.R}{R+(r_{ds_{on}}+R_L)+s(L+R.C.(r_{ds_{on}}+R_L))+R.L.C.s^2} \quad (40)$$

Transfer function from control signal to output is given in (44) by implementing (41), (42) and (43) into (40).

$$G_{d_0} = \frac{v_I R}{R+r_{ds_{on}}+R_L} \quad (41)$$

$$w_0 = \sqrt{\frac{R+r_{ds_{on}}+R_L}{R.L.C}} \quad (42)$$

$$Q = \frac{\sqrt{R.L.C.(R+(r_{ds_{on}}+R_L)}}{L+R.C.(r_{ds_{on}}+R_L)} \quad (43)$$

$$G_{vd} = \frac{G_{d_0}}{1+\frac{s}{Qw_0}+\frac{s^2}{w_0^2}} \quad (44)$$

4. Simulation of Converter and Design of a Conventional PI Controller

In this part of the study, a discrete time PI controller was designed for the converter and its simulations was performed in MATLAB/Simulink. Firstly, system is investigated for ideal case and then transfer function of system given in (40) is discretized and re-converted by Zero-Order-Hold (ZOH) method. A conventional type PI controller is designed and its coefficients are determined by PID Tool in MATLAB/Simulink.

In order to obtain duty ratio of switching devices, output voltage obtained from PI controller function is compared with input voltage. Sampling frequency of the microcontroller is chosen same for both experimental and simulation studies to obtain consistency between the results. Combined model of converter, PI controller and gate signal generator is illustrated in Figure 9.

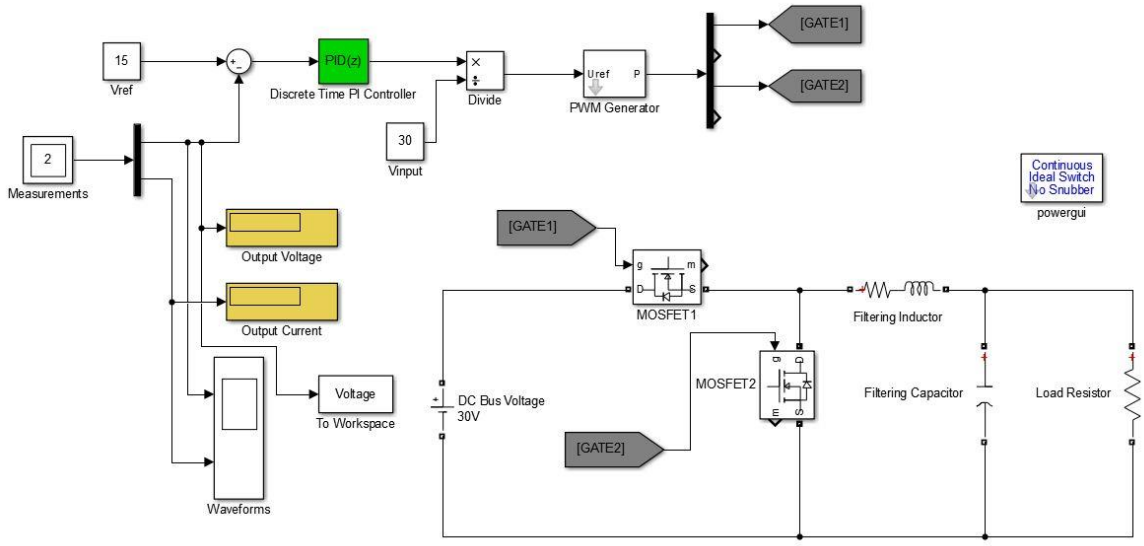

Figure 9. Control to output equivalent circuit.

5. Simulation Results and Stability Analysis

Since, a closed loop control is applied, a feedback path has been used.

Feedback path may lead a stable system to become unstable. Even if the system does not have a pole on the right half, the right half plane pole may appear when the system is transformed into closed loop. Stability analysis is performed on the Bode diagram by passing to frequency domain. The Bode diagram gives information about the amplitude and phase of the system response of the converter according to frequency change [15].

Apart from several exclusive cases, power electronic converters exhibits a critical damping behaviour in case that system contains a right half-plane zero and also when phase gain is between 25° and 45° [7]. However, in the case of small phase gain, the quality factor (Q) in closed loop transfer function increases, which causes the system to overshoot in transient state behaviour.

The open-loop phase gain of the designed converter and variation of the amplitude with frequency is given by the Bode Plot in Figure 10. Although it is seen that the system is stable in open loop operation, the phase gain is not at a sufficient level. The system phase gain is 8.33° and the zero-dB cut-off frequency is 2350 Hz.

If uncontrolled rectifier and a passive filter are used as the input voltage source, the harmonic effects must be examined on the system and controller. It can be seen that the gain of the harmonics at 100 Hz frequency is 28.6 dB. Thus, the system cannot suppress the largest even harmonics at the supply frequency (f) of the rectifier.

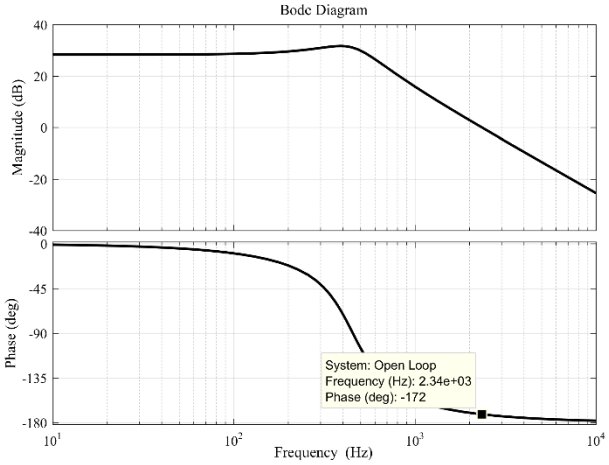

Figure 10. Open-loop bode diagram of converter

In order to observe the transient and the steady state behaviour of the converter, converter and controller are modelled in MATLAB/Simulink. Starting the converter with rated load and with no load, load change and input voltage change in load operation were investigated. The change of output voltages for the scenarios given above are given in Figure 11-16.

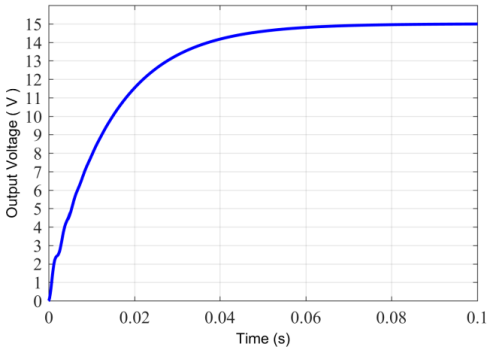

Figure 11. Change of output voltage when system is started with no load

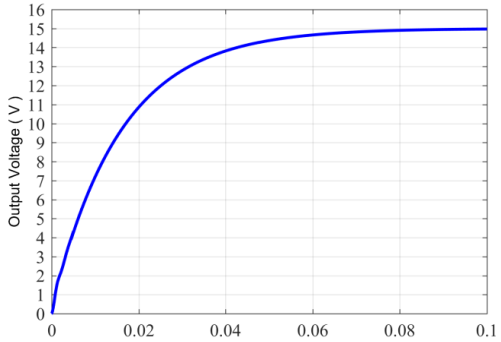

Figure 12. Change of output voltage when starting system with rated load

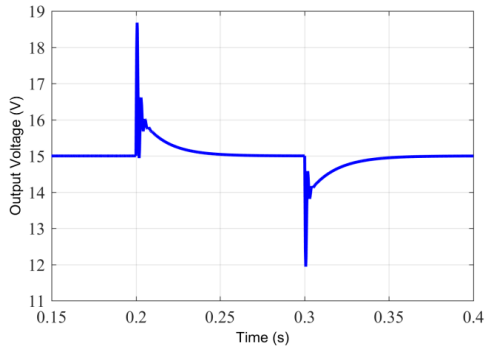

Figure 13. Change of output voltage at re-loading the converter by rated load after reducing the load to 33% which is previously reduced from rated load

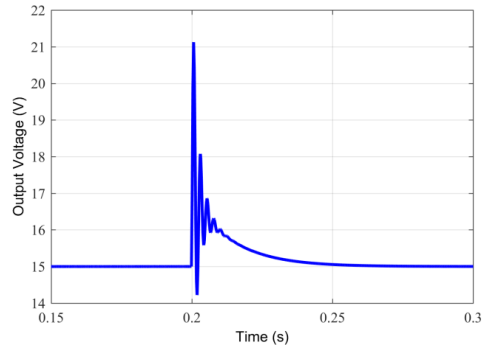

Figure 14. Change of output voltage in case of passing through no-load operation while operating at rated load

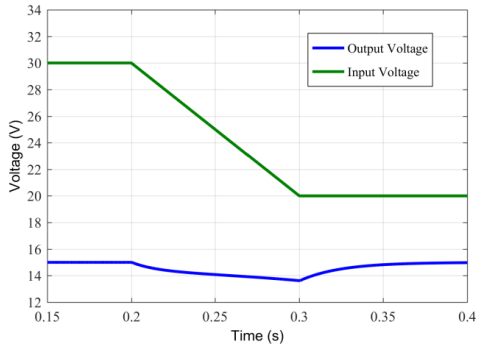

Figure 15. Change of the output voltage when the input voltage of the converter is reduced by 33% while the converter is operating at rated load

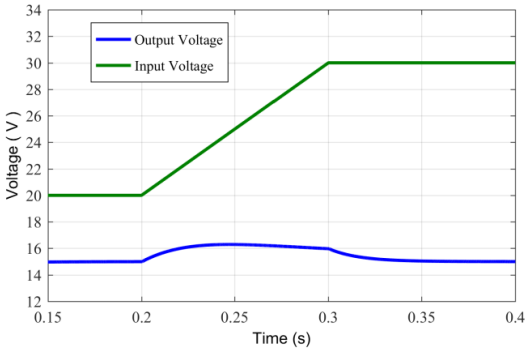

Figure 16. Change of the output voltage when the input voltage of the converter is increased by 50% while the converter is operating at rated load

It can be seen that the system can respond quickly to the change of operating conditions by means of designed controller. The effect of the designed controller on open loop Bode diagram of the converter is given in Figure 17. It is seen that the phase gain is increased from 8.33° to 26.8°, and "Zero dB" cut-off frequency is reduced from 2350 Hz to 649 Hz thanks to designing controller.

The control system amplifies the signals in frequencies up to the cut-off frequency and damps the signals with frequencies greater than this frequency. In order to eliminate the harmonics on converter output voltage created by switching, cutting frequency of controller is reduced.

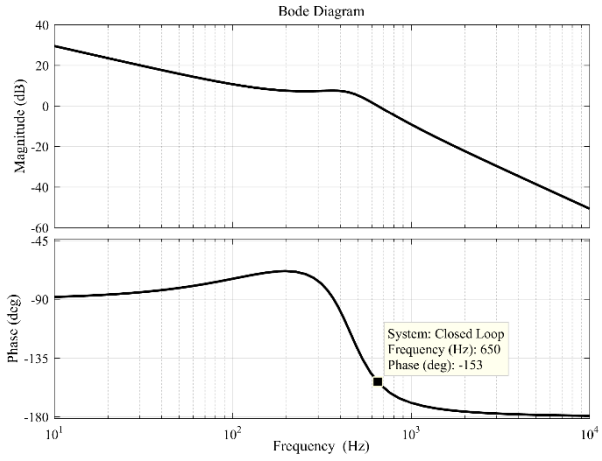

Figure 17. Change of the output voltage when the input voltage of the converter is increased by 50% while the converter is operating at rated load

The gain at 100 Hz dropped to 10.7 dB by means of the controller. The signals at this frequency are suppressed more than that of the uncontrolled state. The system is stable in the closed loop and the designed controller does not cause unstable behaviour in the system.

6. Test Results

The converter was manufactured after completing the design, simulation and stability analysis stages. In order to increase the efficiency of the converter and to eliminate the core losses of inductance, air-core inductance was chosen

instead of ferrite core inductance. IRFZ44N MOSFET is used as switching device and IR2112 is used as MOSFET driver. In order to drive high and low side switching device, "bootstrap" technique was applied [15].

Designed controller was embedded to a microcontroller based digital signal processor entitled C2000 Piccolo LaunchPad and output voltage was controlled. Designed converter and its test set up are illustrated in Figure 18.

During tests, the same operating scenarios used in simulations were examined. The used scenarios for practical tests are "Starting the converter with rated load and with no load", "Re-loading the converter by rated load after reducing the load to 33% which is previously reduced from rated load"," "Unloading suddenly when the converter was operating at rated load", "Reducing the input voltage by 33% and increasing of input voltage by 50% while the converter was operating at rated load". The measured changes of output voltages of the converter are shown in Figure (19)-(24)

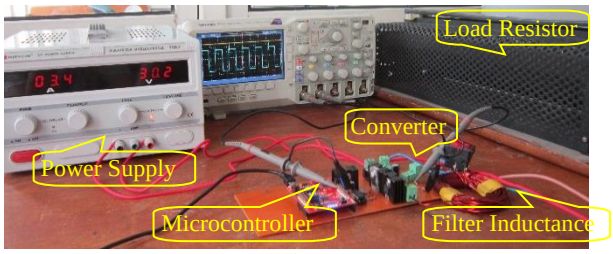

Figure 18. Designed converter and test set up.

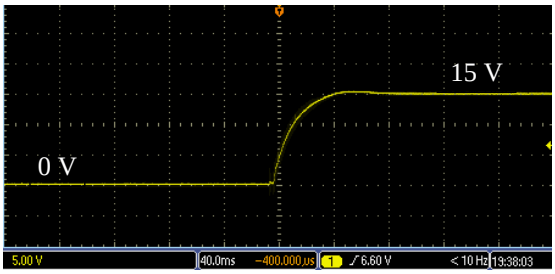

Figure 19. Change of output voltage when system is started with no load (5V/DIV-40ms/TDIV)

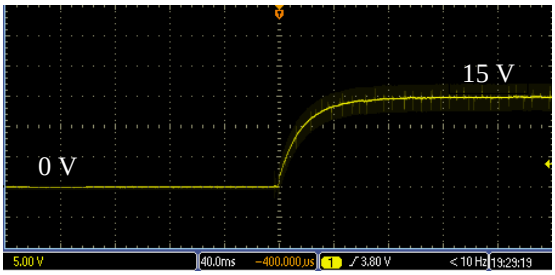

Figure 20. Change of output voltage when starting system with rated load (5V/DIV-40ms/TDIV)

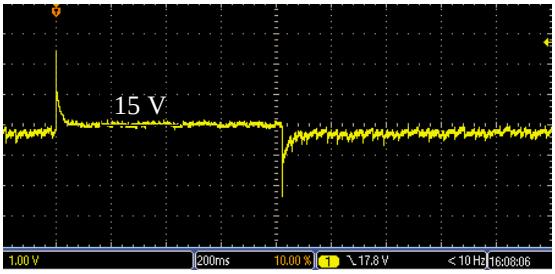

Figure 21. Change of output voltage at re-loading the converter by rated load after reducing the load to 33% which is previously reduced from rated load (1V/Div-200ms/TimeDiv)

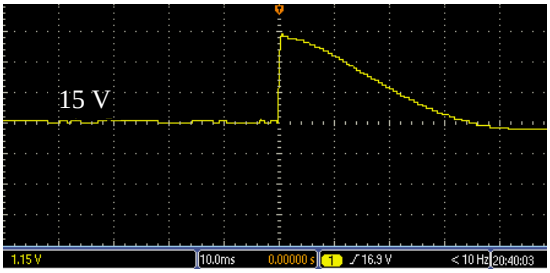

Figure 22. Change of output voltage in case of passing through no-load operation while operating at rated load (1.15V/Div-10ms/TimeDiv-when 15V bias voltage was applied)

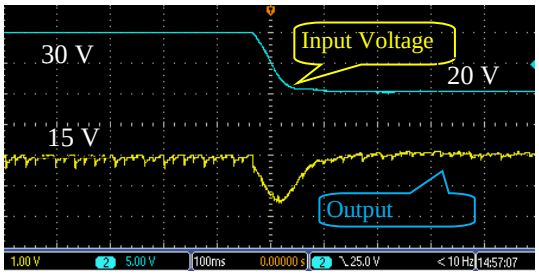

Figure 23. Change of the output voltage when the input voltage of the converter is reduced by 33% while the converter is operating at rated load (input voltage 5V/Div-100ms/TimeDiv, output voltage-1 V/Div-100ms/TimeDiv- when 15V bias voltage was applied)

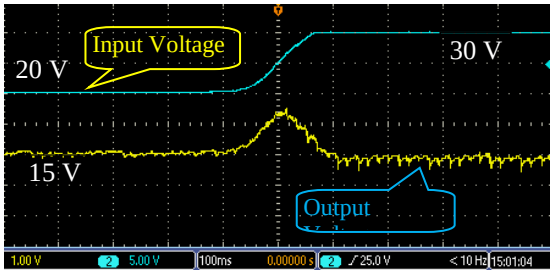

Figure 24. Change of the output voltage when the input voltage of the converter is increased by 50% while the converter is operating at rated load (input voltage 5V/Div-100ms/TimeDiv, output voltage-1 V/Div-100ms/TimeDiv- when 15V bias voltage was applied)

Simulation and test results for starting the converter with rated load for performance comparison of designed controller are given in Table 2.

Table 1. Performance comparison of designed controller

Performance Criteria	Simulation Results	Test Results
Rising Time	0.035 s	0.03608 s
Settling Time	0.0625 s	0.076 s
Overshoot	% 0	% 2.703
Steady State Error	% 0	% 2

7. Conclusion

In this study, non-ideal analysis of a synchronous buck converter is performed. Transfer functions from input voltage to output voltage and from control signal to output voltage are obtained and discretized by MATLAB. On-state resistances of switches and resistance of inductance winding is added to the model during simulation phase. A traditional discrete PI controller is designed for the converter and stability analysis is performed for the system including the designed controller. Results of both simulation and practical study tests are observed in comparison. Same loading scenarios for both simulation and practical study are realised like different starting, loading, load changing and input voltage change conditions. It was seen that simulation and practical study results are extremely equal to each other. With this methodology, "the difference between test and simulation results of an SBC (also any other converter) where ideal power electronic switches and conditions are used in simulations" is eliminated in this study by means of established model and designed controller.

8. References

[1] A. Peterchev, S. Sanders, "Digital Loss Minimizing Multi-Mode Synchronous Buck Converter Control". 2004 35th Annual IEEE Power Electronics Specialists Conference, Aachen, Germany, 20-25 June 2004.

[2] M. Karadeniz, O.M. Gulbahce, D.A. Kocabas. "A practical design and analysis of a high power DC to DC converter". MECHATRONIKA, 2012 15th International Symposium, Prague, Czech Republic, 5-7 December 2012.

[3] G. Suman, B. Kumar, M. Kumar, B. Babu, K. Subhashini. "Modeling, Analysis and Design of Synchronous Buck Converter Using State Space Averaging Technique for PV Energy System". International Symposium on Electronic System Design (ISED), Kolkata, India, 19-22 December 2012.

[4] P.J. Agrawal, "Modeling and simulation of low duty ratio buck synchronous converter under large load current switching". 2013 IEEE 63rd Electronic Components and Technology Conference, Las Vegas, USA, 28-31 May 2013.

[5] B.C. Babu, Sriharsha, A. Kumar, N. Saroagi, R.S Samantaray, "Design and Implementation of Low Power Smart PV Energy System for Portable Applications Using Synchronous Buck Converter". 2011 International Symposium on Electronic System Design (ISED), Kochi, India, 19-21 December 2011.

[6] V.A. Stankovic, L. Nerone, P. Kulkarni. "Modified Synchronous-Buck Converter for a Dimmable HID Electronic Ballast". IEEE Transactions on Industrial Electronics, 59(4), 1815-1824, 2012.

[7] R. Erickson, D. Maksimovic. "Fundamentals of Power Electronics", 2nd ed. New York, Kluwer Academic Publishers, USA, 2001.

[8] C.G. Wilson, J.Y. Hung, R.N. Dean. "A sliding mode controller for two-phase synchronous buck converters". IECON 2012 - 38th Annual Conference on IEEE Industrial Electronics Society, Montreal, QC, 25-28 October 2012.

[9] Y. Yuan, Y. Lv, G. Tong. "Study on the digitally controlled system of ZCS-QRC synchronous buck converter". Control Conference (CCC), Yantai, China, 22-24 July 2011.

[10] C. Chang. "Mixed voltage /current mode control of PWM synchronous buck converter". Power Electronics and Motion Control Conference, Xi'an, China, 14-16 August 2004.

[11] B. Jongbok, C. Wooin, B. Cho. "Digital control of synchronous buck converter with multi-mode for wide load range". Power Electronics and Motion Control Conference (IPEMC), Harbin, China, 2-5 June 2012.

[12] D. Hart, "Power Electronics". 1st ed. New York, McGraw-Hill, USA, 2011.

[13] B. Yildiz, M. O. Gülbahçe and D. A. Kocabaş, "Nonideal analysis and voltage mode control of a synchronous buck converter". National Conference on Electrical, Electronics and Biomedical Engineering (ELECO), Bursa, 2016, pp. 392-396.

[14] J. Kassakian. "Principles of Power Electronics". 1st ed. Utah,, Addison-Wesley, USA, 1991.

[15] Infineon. "HV Floating MOS-Gate Driver ICs". http://www.infineon.com/dgdl/an-978.pdf?fileId=5546d462533600a40153559f7cf21200z (11.10.2016).

[16] G. Altintas, M.O. Gulbahce, D.A. Kocabas "Nonideal Analysis, Design and Voltage Mode Control of a Boost Converter". RTUCON 57th International Scientific Conference on Power and Electrical Engineering of Riga Technical University, Riga, Latvia, 13-14 October 2016.